COVER SHEET

Frost, Ray L. and Musumeci, Anthony W. and Adebajo, Moses and Martens, Wayde (2007) Using thermally activated hydrotalcite for the uptake of phosphate from aqueous media. *Journal of thermal Analysis and Calorimetry* 89(1):pp. 95-99.

Using thermally activated hydrotalcite for the uptake of phosphate from aqueous media

Ray L. Frost[•], **Anthony W. Musumeci, Moses Adebajo and Wayde Martens**

Inorganic Materials Research Program, School of Physical and Chemical Sciences, Queensland University of Technology, GPO Box 2434, Brisbane Queensland 4001, Australia.

Abstract:

Hydrotalcites of formula $Mg_6Al_2(OH)_{16}(PO_4).4H_2O$ formed by intercalation with the phosphate anion as a function of pH show variation in the d-spacing attributed to the size of the hydrated anion in the interlayer. The value changes from 11.91 Å for pH 9.3, to 7.88 Å at pH 12.5. No crystalline hydrotalcites with phosphate in the interlayer were formed at pH 9.3. Thermal decomposition identifies three steps namely dehydration, dehydroxylation and some loss of carbonate during the thermal treatment. The addition of a thermally activated ZnAl-HT to a phosphate solution resulted in the uptake of the phosphate and the reformation of the hydrotalcite. The technology has the potential for water purification through anion removal.

Keywords: nanochemistry, thermally activated hydrotalcite, phosphate removal, pyroaurite, thermal analysis

Introduction

Hydrotalcites, or layered double hydroxides (LDH's) are fundamentally anionic clays, and are less well-known than cationic clays like smectites [1, 2]. The structure of hydrotalcite can be derived from a brucite structure ($Mg(OH)_2$) in which e.g. Al^{3+} or Fe^{3+} (pyroaurite-sjögrenite) substitutes a part of the Mg^{2+} [3-14]. This substitution creates a positive layer charge on the hydroxide layers, which is compensated by interlayer anions or anionic complexes [15, 16]. When LDHs are synthesized any appropriate anion can be placed in the interlayer. These anions may be any anion with a suitable negative charge including the phosphate anion. The hydrotalcite may be considered as a gigantic cation which is counterbalanced by anions in the interlayer. In hydrotalcites a broad range of compositions are possible of the type $[M^{2+}_{1-x}M^{3+}_x(OH)_2][A^{n-}]_{x/n}.yH_2O$, where M^{2+} and M^{3+} are the di- and trivalent cations in the octahedral positions within the hydroxide layers with x normally between 0.17 and 0.33. It is normal practice to determine the composition of the formed hydrotalcite by chemical means such as ICP-AES or EDAX techniques. A^{n-} is an exchangeable interlayer anion [17]. In the hydrotalcites reevesite and pyroaurite, the divalent cations are Ni^{2+} and Mg^{2+} respectively with the trivalent cation being Fe^{3+}. In these cases, the carbonate anion is the major interlayer counter anion. Normally the hydrotalcite structure based upon takovite (Ni,Al) and hydrotalcite (Mg,Al) has basal spacings of ~8.0 Å where the interlayer anion is carbonate.

[•] Author to whom correspondence should be addressed (r.frost@qut.edu.au)

Reevesite and pyroaurite are based upon the incorporation of carbonate into the interlayer with d(001) spacings of around 8 Å [18, 19].

Thermal analysis using thermogravimetric techniques enables the mass loss steps, the temperature of the mass loss steps and the mechanism for the mass loss to be determined [6, 11, 20-24]. Thermoanalytical methods provide a measure of the thermal stability of the hydrotalcite. The reason for the potential application of hydrotalcites as catalysts rests with the ability to make mixed metal oxides at the atomic level, rather than at a particle level. Such mixed metal oxides are formed through the thermal decomposition of the hydrotalcite [25, 26]. There are many other important uses of hydrotalcites such as in the removal of environmental hazards in acid mine drainage [27, 28], and a mechanism for the disposal of radioactive wastes [29]. Their ability to exchange anions presents a system for heavy metal removal from contaminated waters [30]. Structural information on different minerals has successfully been obtained recently by sophisticated thermal analysis techniques [6, 20-24]. In this work we report the thermal analysis of hydrotalcite with phosphate in the interlayer and explore the effect of pH on hydrotalcite formation.

Experimental

Synthesis of hydrotalcite compounds:

A mixed solution of aluminium and magnesium nitrates ($[Al^{3+}]$ = 0.25M and $[Mg^{2+}]$ = 0.75M; 1M = 1mol/dm^3) and a mixed solution of sodium hydroxide ($[OH^-]$ = 2M) and the desired anion, at the appropriate concentration, were placed in two separate vessels and purged with nitrogen for 20 minutes (all compounds were dissolved in freshly decarbonated water). The cationic solution was added to the anions via a peristaltic pump at 40mL/min and the pH maintained above 9. The mixture was then aged at 75°C for 18 hours under a N_2 atmosphere. The resulting precipitate was then filtered thoroughly, with room temperature decarbonated water to remove nitrates and left to dry in a vacuum desiccator for several days. In this way hydrotalcites with different anions in the interlayer were synthesised. The phase composition was checked by X-ray diffraction and the chemical composition by EXA analyses.

Phosphate uptake from thermally activated Zinc/Aluminium hydrotalcite initially containing carbonate in the interlayer was also studied. The $Zn_6Al_2(OH)_{16}(CO_3).4H_2O$ hydrotalcite was thermally activated by heating to 235°C and kept in a sealed, dry container to minimise absorption of CO_2 and water vapour from the air reforming the clay like structure. The thermally activated powder (3g) was then placed in a 0.1M Tri-sodium orthophosphate solution (five fold excess). The mixture was stirred continuously and aliquots of the solution were taken at intervals from 30 min - 6 hours, filtered and dried before subsequent analysis.

X-ray diffraction

X-Ray diffraction patterns were collected using a Philips X'pert wide angle X-Ray diffractometer, operating in step scan mode, with Cu K_α radiation (1.54052 Å). Patterns were collected in the range 3 to 90° 2θ with a step size of 0.02° and a rate of

30s per step. Samples were prepared as a finely pressed powder into aluminium sample holders.

Thermal Analysis

Thermal decompositions of the hydrotalcites were carried out in a TA® Instruments incorporated high-resolution thermogravimetric analyzer (series Q500) in a flowing nitrogen atmosphere (80 cm^3/min). Approximately 50mg of sample was heated in an open platinum crucible at a rate of 2.0 °C/min up to 500°C. The TGA instrument was coupled to a Balzers (Pfeiffer) mass spectrometer for gas analysis. Only selected gases were analyzed.

Results and discussion

X-ray diffraction

The X-ray diffraction patterns for the phosphate interlayered hydrotalcites are shown in Figure 1. Hydrotalcite normally has a d(003) spacing of 7.9 Å. The sulphate interlayered hydrotalcite has a spacing of 7.99 Å. The XRD patterns show that the d-spacing for the phosphate interlayered hydrotalcite is pH dependent. The hydrotalcite formed at pH 9.3 shows amorphicity. However the d(003) spacing can be still determined as 11.91 Å. The d-spacing for the pH=11.9 formed hydrotalcite is 8.04 Å and the value for the phosphate interlayered hydrotalcite at pH 12.5 is 7.88 Å. Such values are close to the d-spacing values reported for the natural hydrotalcite with sulphate in the interlayer. The decreased interlayer spacing is attributed to the reduction in size of the hydrated phosphate anion between the brucite-like layers. Because of the uncertainty of the complete formation of the phosphate interlayered hydrotalcite formed at pH 9.3, the thermal decomposition was not studied further. The products of the thermal decomposition of the phosphate interlayered hydrotalcite are MgO and $MgAl_2O_4$ (spinel). This observation means that the phosphate is lost during the thermal decomposition process.

Thermogravimetric analysis

The thermogravimetric analysis of the phosphate interlayered hydrotalcite formed at pH=11.9 is shown in Figure 2. The ion current curves for the evolved gases are reported in Figure 3. In the DTG pattern three mass loss steps are observed at 38, 162 and 355 °C with mass losses of 23.7, 11.9 and 15.0 %. The first mass loss step is attributed to the loss of adsorbed water and some dehydration. The second mass loss at 162 °C is ascribed to dehydration and the mass loss at 355 °C to dehydroxylation. By using a formula $Mg_6Al_2(OH)_{16}(HPO_4).4H_2O$, calculations show that the theoretical mass losses for dehydration , dehydroxylation and the loss of phosphate are 11.3, 22.6 and 11.15 %. The experimental mass loss at 38 °C is twice the theoretical value. In this case the number of water units in the formula is estimated to be 8. i.e. according to the TG results the formula of this hydrotalcite should be written as $Mg_6Al_2(OH)_{16}(HPO_4).8H_2O$.

The ion current curves show the mass of evolved water vapour as a function of temperature. The ion current curves for mass of 17 (OH) and 18 (H_2O) show that water vapour is evolved at 40, 163 and 354 °C. The ion current curve for mass = 44

(CO_2) shows that some carbon dioxide was evolved during the thermal decomposition. The presence of CO_2 means that some carbonate anion was incorporated into the interlayer as well as the phosphate anion. Despite taking all the relevant precautions CO_2 gets into the synthesis route of the phosphate interlayered hydrotalcite. Another possibility is that some phosphate is exchanged for CO_2 as a solid state reaction after the phosphate interlayered hydrotalcite has been formed. The hydrophosphate anion ends up as a hydrophosphonic acid.

$$Mg_6Al_2(OH)_{16}(HPO_4).8H_2O + CO_2 \rightarrow Mg_6Al_2(OH)_{16}(HPO_4)_{0.5}(CO_3)_{0.5}.8H_2O + (HPO_4)^{2-}$$

The Thermal decomposition of hydrotalcite with phosphate in the interlayer formed at pH = 12.5 is shown in Figure 4. The ion current curves for the evolved gases are reported in Figure 5. In the DTG pattern three mass loss steps are observed over the 25 to 190 temperature range, at 338 and 391 °C with mass losses of 16.5, 12.4 and 8.4 %. A further mass loss is observed at 455 °C of 3.2 %. As above by using a formula $Mg_6Al_2(OH)_{16}(HPO_4).4H_2O$, calculations show that the theoretical mass losses for dehydration , dehydroxylation and the loss of phosphate are 11.3, 22.6 and 11.15 %. The ion current curves show that water is lost up to 150 °C. OH units are lost at 343 and 393 °C. No water is lost above these temperatures. Some carbon dioxide is lost at 305, 393 and 448 °C (please note a scaling factor of 25 in Figure 5).

The hydrotalcite $Mg_6Al_2(OH)_{16}(CO_3).4H_2O$ is thermally activated by heating to above the decomposition temperature of around 235 °C. It should be noted that it is the carbonate interlayered hydrotalcite which is used as the starting material for phosphate removal. This temperature of ~235°C was chosen based upon the thermal analysis results for the thermal decomposition of the carbonate interlayered hydrotalcite. . If the hydrotalcite is activated to a higher temperature then magesium oxide is formed which may not entirely go back to the hydrotalcite upon reaction with any appropriate anion, in this case the phosphate anion. These results show that dehydration, dehydroxylation and loss of carbonate steps have occurred by this temperature. The thermal activation of the hydrotalcite results in the destruction of the layered structure.

Upon addition of the thermally activated hydrotalcite to an aqueous solution containing phosphate anions the so-called ‘memory’ effect of hydrotalcites comes into play. Hydrotalcites after thermal decomposition will regain their original structure providing the compound is not heated to too high a temperature. This effect may be observed in Figure 6 where the XRD pattern of a hydrotalcite is restored after only thirty minutes. Additional peaks are observed and a large d-spacing of d(003) of 10.7 Å is observed for the first hour of exposure. A second d(003) spacing is observed at 7.6 Å. At the 1 hour exposure of the thermally activated MgAl hydrotalcite two d(003) spacings of 10.6 and 7.5 Å are observed. The d-spacing of 10.6 Å is lost after 1 hour. At 2 hours the d(003) spacing is 7.527 Å and at 4 hours the spacing is 7.530 Å. The XRD pattern for the reformed hydrotalcite does not change on further exposure to the aqueous media. The d(003) spacing of 7.5 Å is observed. This means that the thermally activated phosphate anion has incorporated the phosphate into the interlayer of the hydrotalcite structure. This chemistry provides a mechanism for the uptake of phosphate from aqueous solution.

Conclusions

This research has shown that

a) Phosphate can be intercalated into a hydrotalcite as the counter anion.
b) This intercalation is pH dependent
c) The pH determines the nature of the anion in the interlayer
d) Thermally activated hydrotalcite may be used to remove phosphate from an aqueous system.
e) Thermal analysis is used to determine the appropriate temperature for the thermal activation of the HT.
f) Thermally activate hydrotalcites may be used to purify water of inappropriate anions.

Acknowledgements

The financial and infra-structure support of the Queensland University of Technology Inorganic Materials Research Program of the School of Physical and Chemical Sciences is gratefully acknowledged. The Australian Research Council (ARC) is thanked for funding the thermal analysis facility.

References

1. K. Hashi, S. Kikkawa and M. Koizumi, Clays and Clay Minerals 31 (1983) 152.
2. L. Ingram and H. F. W. Taylor, Mineralogical Magazine and Journal of the Mineralogical Society (1876-1968) 36 (1967) 465.
3. J. T. Kloprogge, L. Hickey and R. L. Frost, Materials Chemistry and Physics 89 (2005) 99.
4. L. Frost Ray and L. Erickson Kristy, Spectrochimica acta. Part A, Molecular and biomolecular spectroscopy 61 (2005) 51.
5. K. L. Erickson, T. E. Bostrom and R. L. Frost, Materials Letters 59 (2004) 226.
6. R. L. Frost and K. L. Erickson, Journal of Thermal Analysis and Calorimetry 76 (2004) 217.
7. R. L. Frost and K. L. Erickson, Thermochimica Acta 421 (2004) 51.
8. J. T. Kloprogge, L. Hickey and R. L. Frost, Journal of Raman Spectroscopy 35 (2004) 967.
9. J. T. Kloprogge, L. Hickey and R. L. Frost, Journal of Solid State Chemistry 177 (2004) 4047.
10. R. L. Frost and Z. Ding, Thermochimica Acta 405 (2003) 207.
11. R. L. Frost, W. Martens, Z. Ding and J. T. Kloprogge, Journal of Thermal Analysis and Calorimetry 71 (2003) 429.
12. R. L. Frost, M. L. Weier, M. E. Clissold and P. A. Williams, Spectrochimica Acta, Part A: Molecular and Biomolecular Spectroscopy 59 (2003) 3313.
13. R. L. Frost, M. L. Weier, M. E. Clissold, P. A. Williams and J. T. Kloprogge, Thermochimica Acta 407 (2003) 1.
14. R. L. Frost, M. L. Weier and J. T. Kloprogge, Journal of Raman Spectroscopy 34 (2003) 760.
15. R. M. Taylor, Clay Minerals 17 (1982) 369.
16. H. F. W. Taylor, Mineralogical Magazine and Journal of the Mineralogical Society (1876-1968) 37 (1969) 338.
17. H. C. B. Hansen and C. B. Koch, Applied Clay Science 10 (1995) 5.
18. D. L. Bish and A. Livingstone, Mineralogical Magazine 44 (1981) 339.
19. E. H. Nickel and R. M. Clarke, American Mineralogist 61 (1976) 366.
20. E. Horvath, J. Kristof, R. L. Frost, N. Heider and V. Vagvoelgyi, Journal of Thermal Analysis and Calorimetry 78 (2004) 687.
21. R. L. Frost, M. L. Weier and K. L. Erickson, Journal of Thermal Analysis and Calorimetry 76 (2004) 1025.
22. R. L. Frost and K. L. Erickson, Journal of Thermal Analysis and Calorimetry 78 (2004) 367.
23. E. Horvath, J. Kristof, R. L. Frost, A. Redey, V. Vagvolgyi and T. Cseh, Journal of Thermal Analysis and Calorimetry 71 (2003) 707.
24. J. Kristof, R. L. Frost, J. T. Kloprogge, E. Horvath and E. Mako, Journal of Thermal Analysis and Calorimetry 69 (2002) 77.
25. F. Rey, V. Fornes and J. M. Rojo, J. Chem. Soc., Faraday Trans. 88 (1992) 2233.

26. M. Valcheva-Traykova, N. Davidova and A. Weiss, J. Mater. Sci. 28 (1993) 2157.
27. G. Lichti and J. Mulcahy, Chemistry in Australia 65 (1998) 10.
28. Y. Seida and Y. Nakano, Journal of Chemical Engineering of Japan 34 (2001) 906.
29. Y. Roh, S. Y. Lee, M. P. Elless and J. E. Foss, Clays and Clay Minerals 48 (2000) 266.
30. Y. Seida, Y. Nakano and Y. Nakamura, Water Research 35 (2001) 2341.

List of Figures

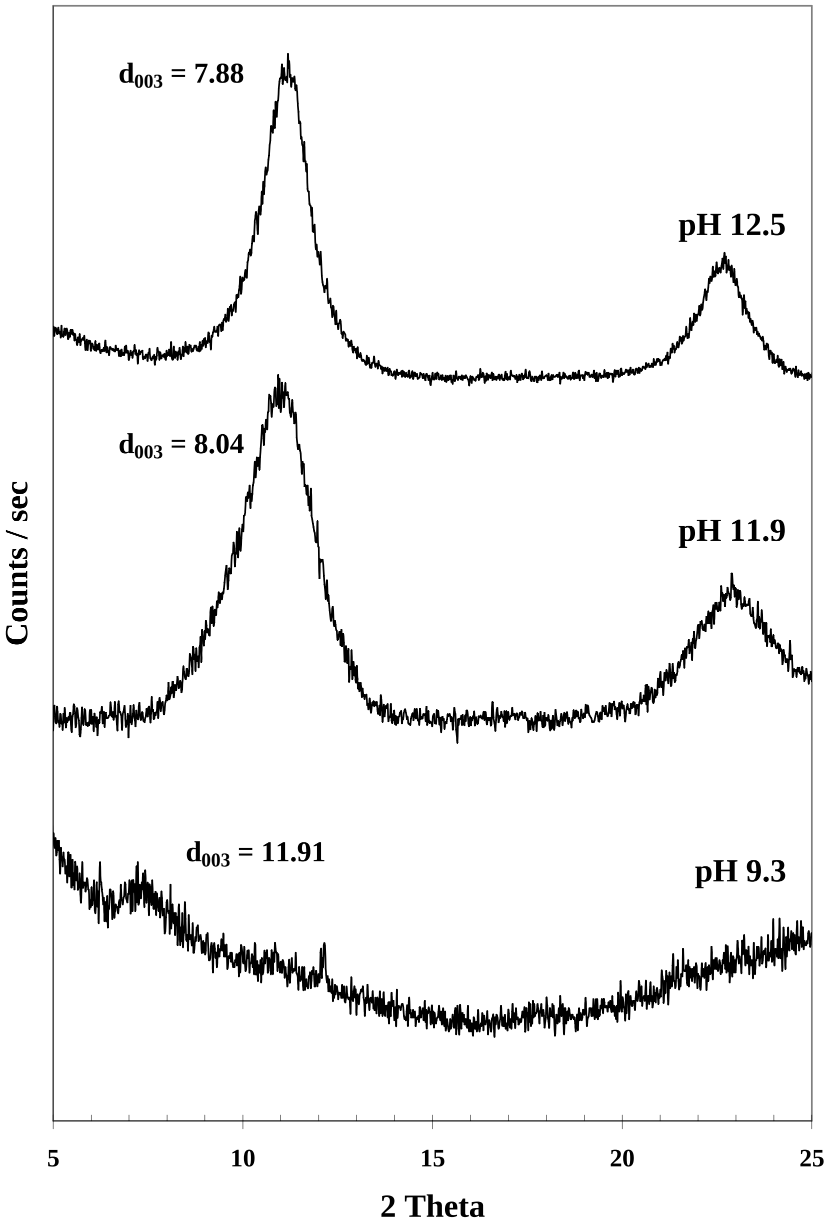
d_{003} = 7.88
pH 12.5
d_{003} = 8.04
pH 11.9
d_{003} = 11.91
pH 9.3
Counts / sec
5
10
15
20
25
2 Theta

Figure 1

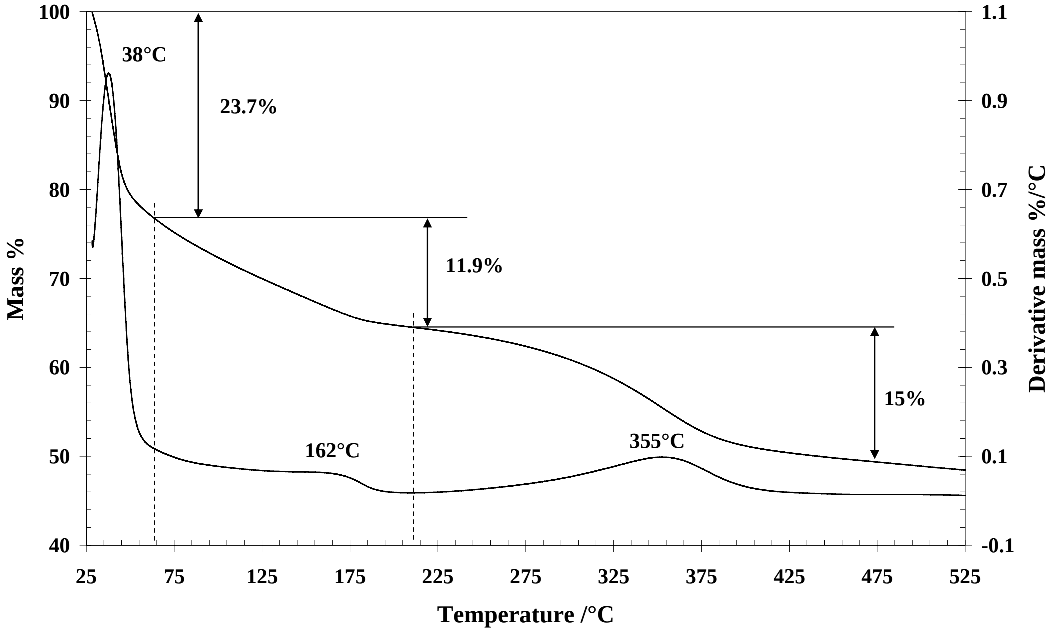

Figure 2 phosphate pH=11.9

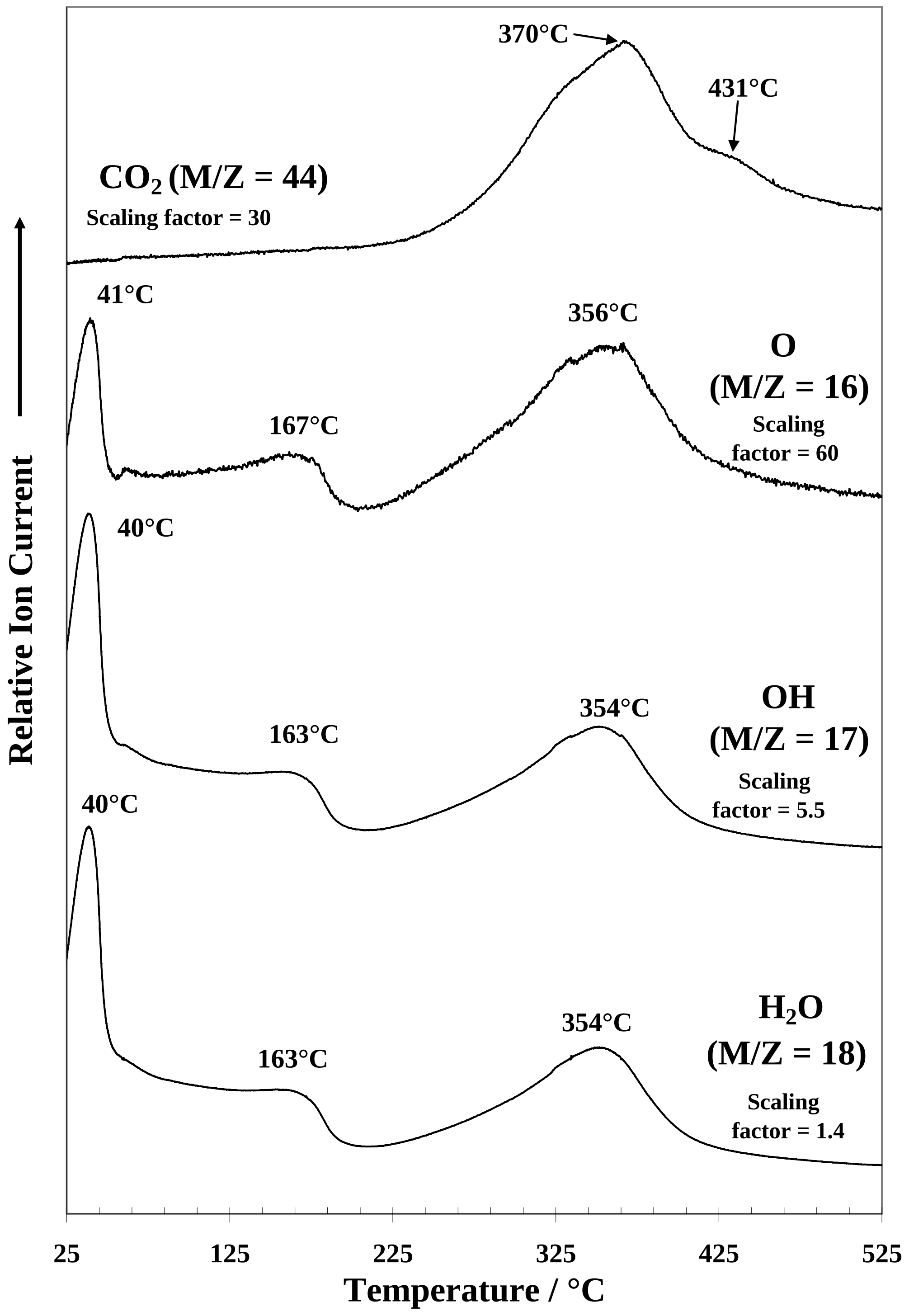

Figure 3 phosphate pH=11.9

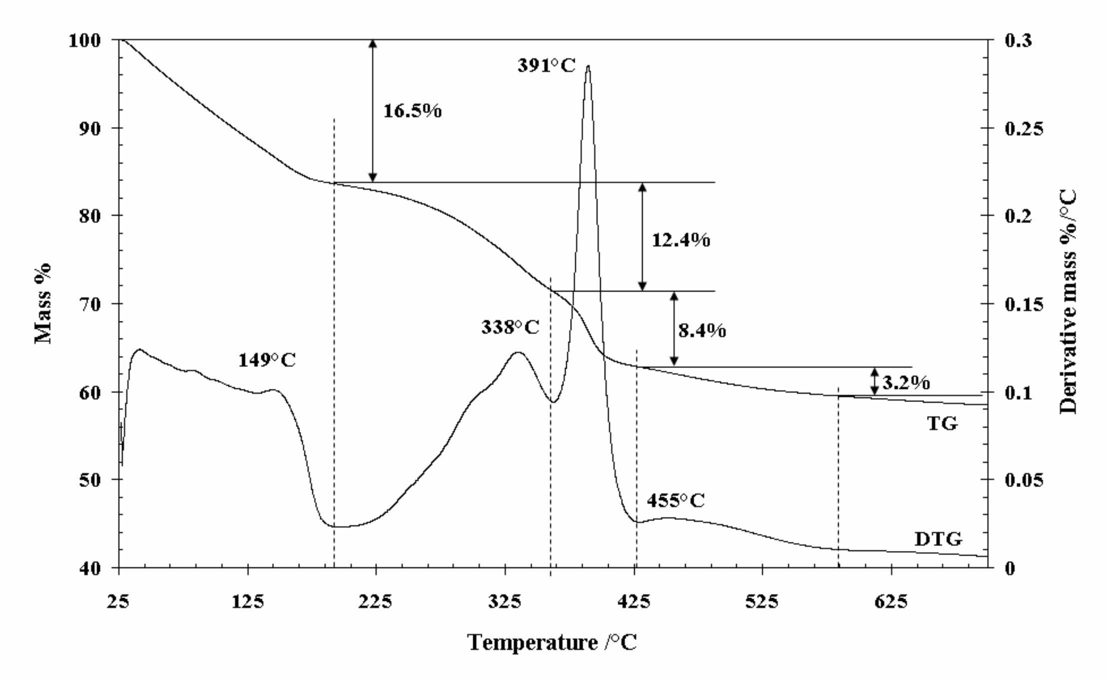

Figure 4 12.5 pH

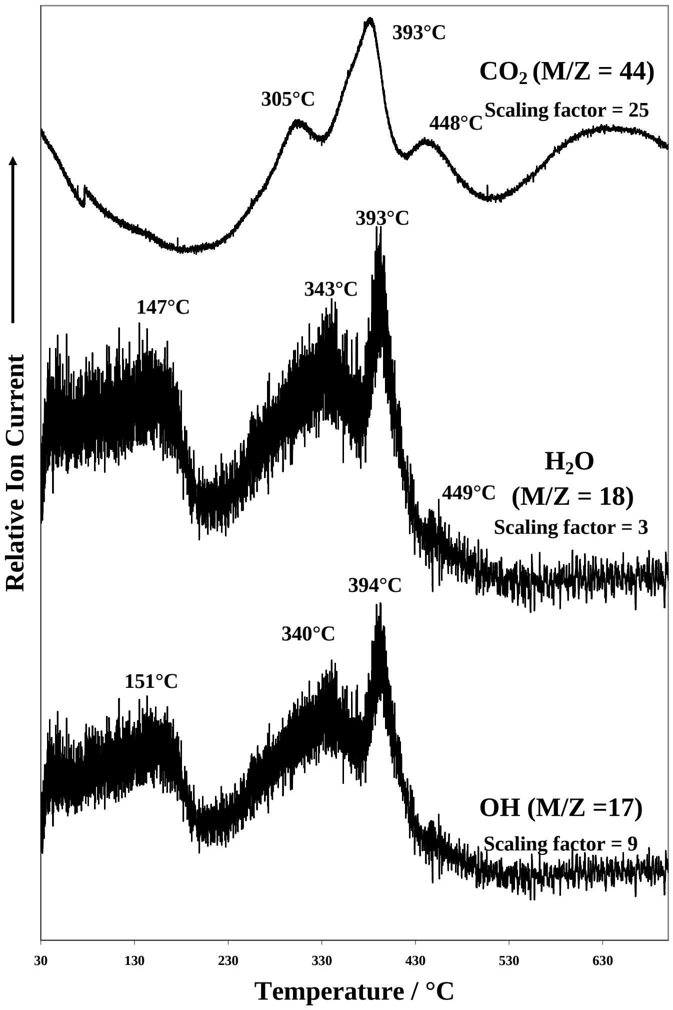
393°C
CO$_2$ (M/Z = 44)
305°C
Scaling factor = 25
448°C
393°C
343°C
147°C
H$_2$O
(M/Z = 18)
449°C
Scaling factor = 3
394°C
340°C
151°C
OH (M/Z =17)
Scaling factor = 9
Relative Ion Current
30
130
230
330
430
530
630
Temperature / °C

Figure 5

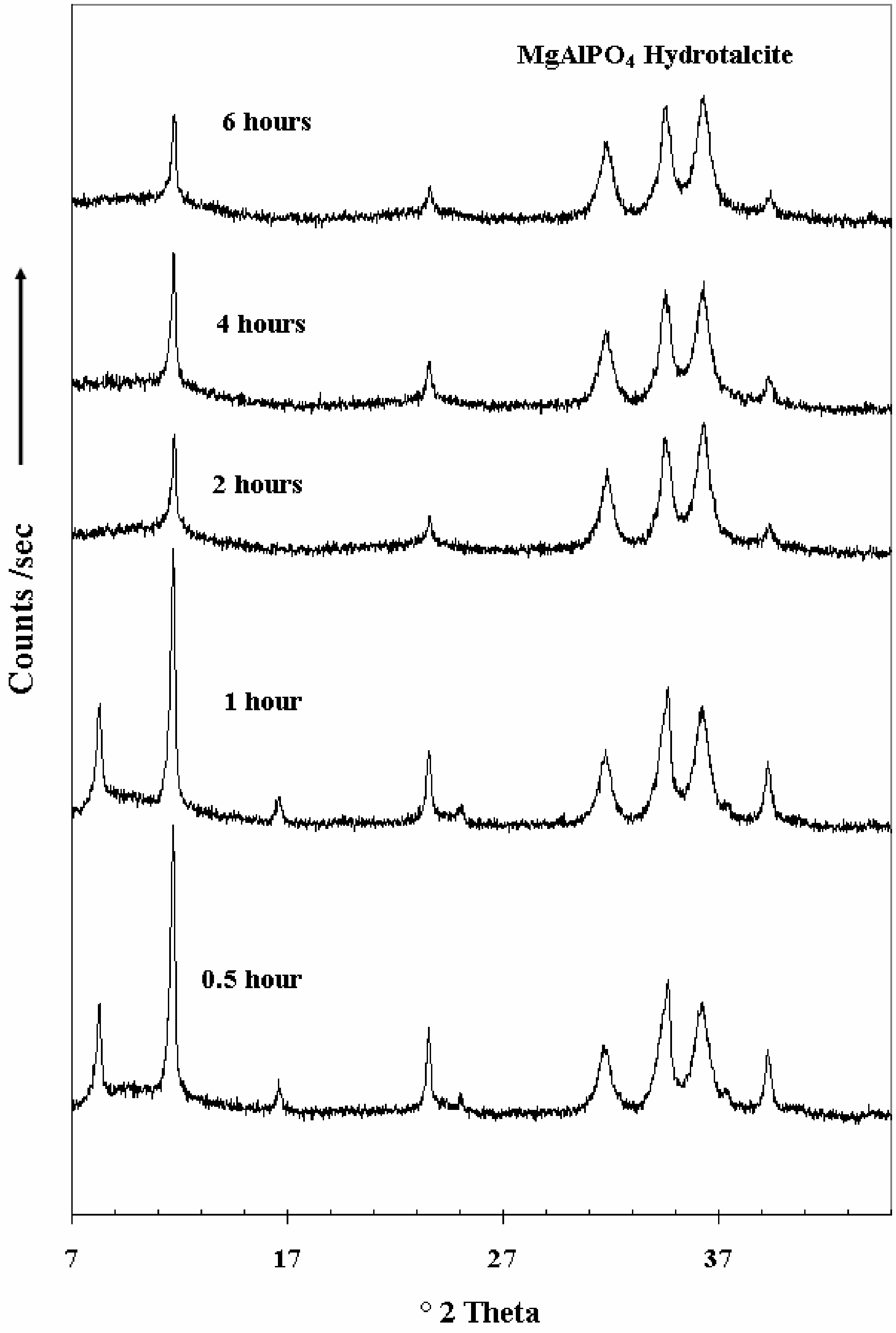
MgAlPO$_4$ Hydrotalcite
6 hours
4 hours
2 hours
1 hour
0.5 hour
Counts /sec
7
17
27
37
° 2 Theta

Figure 6